

Multiple-frame photography for extended depth of field

Jorge Ojeda-Castañeda,^{1,*} Emmanuel Yepez-Vidal,¹ and Cristina M. Gómez-Sarabia²

¹Electronics Department, Engineering Division, University of Guanajuato, Carretera a Valle, Salamanca 36885, Mexico

²Digital Arts, Engineering Division, University of Guanajuato, Carretera a Valle, Salamanca 36885, Mexico

*Corresponding author: jorge_ojedacastaneda@yahoo.com

Received 2 November 2012; revised 27 February 2013; accepted 4 March 2013;
posted 11 March 2013 (Doc. ID 179181); published 0 MONTH 0000

For extending the depth of field, we analyze the result of superimposing several snapshots, which are taken while changing the amount of focus error, at full pupil aperture. We unveil the use of a varifocal lens for controlling the amount of focus error, without modifying either the lateral magnification or light throughput. After recording a set of snapshots, we use suitable acquisition factors for shaping an optical transfer function, which has reduced sensitivity to focus errors. © 2013 Optical Society of America

OCIS codes: 110.4850, 110.4100, 110.1758, 110.688, 110.6915, 070.7425.

1. Introduction

Several authors have described techniques for extending the depth of field of an optical system, which works under noncoherent illumination. These techniques usually have two stages. Typically, in the first stage, one acquires a single image with an optical system that employs a suitable preprocessing mask [1–25]. At the second stage, the recorded pictures are digitally postprocessed for obtaining the final image. Heuristically speaking, these techniques reduce first the influence of focus error on the modulation transfer function (MTF). In this manner, the preprocessing mask ensures that several planar scenes, located at different depths of the object field, suffer from virtually the same amount of contrast reduction. Then, at the postprocessing stage, the image contrast can be simultaneously corrected for all the recorded scenes.

For reducing the impact of focus errors, it is convenient to keep in mind the criteria summarized in Table 1. The columns of Table 1 are arranged as follows. Along column 1, in line 1, we depict schematically the classical technique of narrowing the initial pupil aperture, with cutoff spatial frequency Ω , to a pupil aperture with cutoff spatial frequency $\varepsilon\Omega$, where $0 \leq \varepsilon < 1$. In line 2, we depict schematically

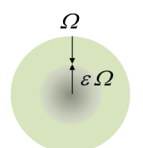
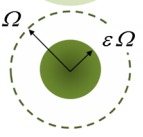
the use of an obscure disk, on-axis, with radial spatial frequency $\varepsilon\Omega$. Along column 2, we write the expressions for the light throughput as a function of ε . Along column 3, we write the Rayleigh tolerance to focus error.

Next, we note in Table 2 that several proposals go far beyond Rayleigh tolerance criteria. For this type of applications, one uses rectangular apertures rather than circular apertures. And rather than using the Rayleigh criteria, one uses criteria based on the MTF [26]. In Table 2, along line 1, we show the interferograms of a rectangular pupil, as we change the focus error coefficient. Along line 2, we display the PSF as focus error increases. And along lines 3 and 4, we display the impact of focus error on two different types of images.

Fifty years ago, Haeusler indicated the usefulness of superimposing several images, in the same photographic plate, while moving the optical system [27]. Furthermore, it has been indicated that it is useful to modulate the exposure time when taking several pictures [28].

Here, our aim is to present a simple mathematical analysis that describes a low cost optical technique for extending the depth of field at full pupil aperture. In other words, based on idealized computer simulations and simple mathematical considerations, we explore the possibility of extending the depth of field by superimposing, with suitable weighting factors,

Table 1. Classical Trade-Offs for Extending the Depth of Focus

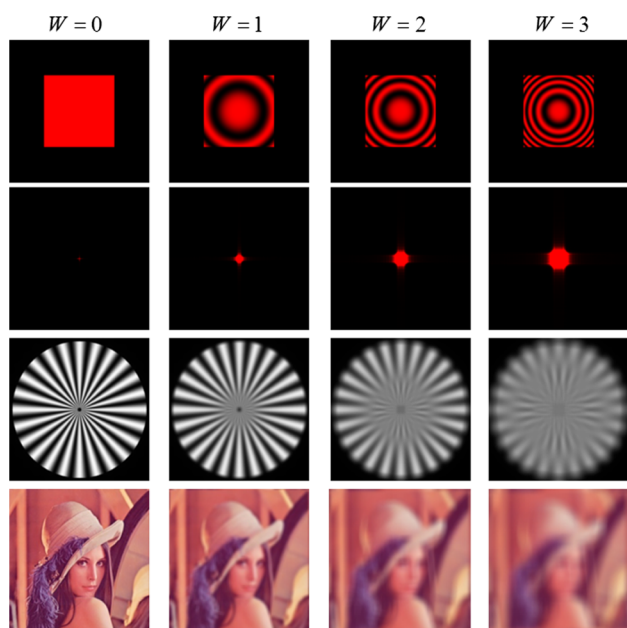
| | T | $W_{2,0} \leq$ |
|---|------------------|-------------------------------------|
|  | ϵ^2 | $\frac{\lambda}{4\epsilon^2}$ |
|  | $1 - \epsilon^2$ | $\frac{\lambda}{4(1 - \epsilon^2)}$ |

T1:1

several snapshots of the same input. Our proposal does not include state-of-the-art techniques for digital recording and processing. Furthermore, even when our mathematical model takes into account the presence of noise, our proposal does not dwell on statistical optics.

In Section 2, we discuss a simple mathematical model that describes the process of taking and averaging several snapshots. At every snapshot, one changes the axial separation between the input plane and a fixed output plane. To that end, in Section 3, we unveil a method that employs a varifocal lens at the Fraunhofer plane of an optical processor [29–32]. This novel method preserves unit magnification in an optical processor, which remains at a fixed position. Once the snapshots are recorded, we add those pictures by using suitable weights. We show that these weights are useful for engineering the optical transfer function (OTF). In Section 4, we make

Table 2. Impact of Focus Error: (a) Interferograms of the Pupil Function, (b) PSF, (c) Siemen Star Images, and (d) Lena Images



T2:1

some useful comparisons. We indicate that if in the Fourier domain the noise is a wide-sense stationary process, then the additive noise averages to a constant value. In Section 5, we illustrate our proposal by discussing two simple examples. If in the Fourier domain the noise is white, then we suggest using Hopkins tolerance formalism for setting a threshold value. Finally, in Section 6, we summarize our discussion with some remarks on the advantages and limitations of our proposal.

2. Acquisition Function

As depicted in Fig. 1, we consider a classical optical processor. We assume that the optical system has a rectangular pupil aperture. For the sake of clarity, our discussion is restricted to the one-dimensional case. The optical processor is represented by its OTF $H_Q(\mu; W)$. We use the subindex Q for indicating that the complex amplitude transmittance of the pupil aperture is $Q(\mu)$. Consequently, the generalized pupil function is

$$P(\mu; W_{2,0}) = Q(\mu) \exp \left[i2\pi W \left(\frac{\mu}{\Omega} \right)^2 \right] \text{rect} \left(\frac{\mu}{2\Omega} \right). \quad (1)$$

In Eq. (1) W is a shorthand notation for describing the presence of the focus error coefficient measured in units of wavelengths. Except for a normalization factor, the OTF is equal to

$$H_Q(\mu; W) = \int_{\frac{-(2\Omega - |\mu|)}{2}}^{\frac{(2\Omega - |\mu|)}{2}} Q \left(\nu + \frac{\mu}{2} \right) Q^* \left(\nu - \frac{\mu}{2} \right) e^{i2\pi \left(\frac{2\nu}{\Omega^2} \right) W} d\nu. \quad (2)$$

For a particular value of W , the recorded irradiance distribution is

$$I(x; W) = \int_{-\infty}^{\infty} \tilde{I}_0(\mu) \cdot H_Q(\mu; W) e^{i2\pi x \mu} d\mu + |N(x; W)|^2. \quad (3)$$

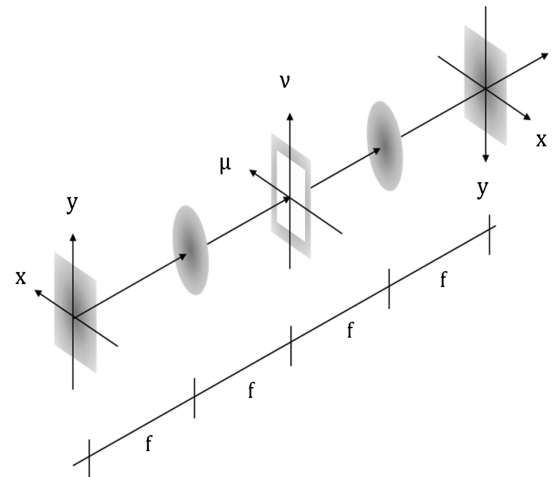


Fig. 1. Schematic diagram of an optical processor.

F1:1

In Eq. (3) the function $\tilde{I}_0(\mu)$ denotes the Fourier spectrum of the input irradiance distribution $I_0(x)$. The function $|N(x; W)|^2$ represents the presence of additive noise at the recording process for a given value of W . Here it is relevant to recognize that W may be treated as a random variable. Next, we define the following ensemble average over the random variable W . That is,

$$\langle I(x) \rangle = \int_{-\infty}^{\infty} g(W) I(x; W) dW. \quad (4)$$

For performing an average, in Eq. (4), we employ a weighting function $g(W)$, which is here denoted as the *acquisition function*. It represents the amplitude weighting factor that one wishes to assign to a snapshot at a random value of W . Hence, heuristically $g(W)$ plays the role of a probability density function. In what follows Eq. (5) puts into effect this viewpoint. By using Eqs. (3) and (4) we have

$$\begin{aligned} \langle I(x) \rangle &= \int_{-\infty}^{\infty} \tilde{I}_0(\mu) \int_{-\infty}^{\infty} g(W) H_Q(\mu; W) dW e^{i2\pi x \mu} d\mu \\ &+ \int_{-\infty}^{\infty} g(W) |N(x; W)|^2 dW \\ &= \int_{-\infty}^{\infty} \tilde{I}_0(\mu) \langle H_Q(\mu) \rangle e^{i2\pi x \mu} d\mu + \langle |N(x)|^2 \rangle. \end{aligned} \quad (5)$$

In Eq. (5) we denote as $\langle |N(x)|^2 \rangle$ the ensemble average of the additive noise $N(x; W)$. In Appendix A, we show that for a wide-sense stationary process, $\langle |N(x)|^2 \rangle = N_0$, which is a constant. In Section 4, we discuss the presence of white noise. Now, from Eq. (5) we have

$$\langle I(x) \rangle - \langle |N(x)|^2 \rangle = \int_{-\infty}^{\infty} \tilde{I}_0(\mu) \langle H_Q(\mu) \rangle e^{i2\pi x \mu} d\mu. \quad (6)$$

It is apparent from Eq. (6) that in principle one can recover the initial Fourier spectrum, $\tilde{I}_0(\mu)$. To that end, we recognize the need for having $\langle H_Q(\mu) \rangle \neq 0$. If this requirement is met, then

$$\tilde{I}_0(\mu) = [\langle H_Q(\mu) \rangle]^{-1} \int_{-\infty}^{\infty} [\langle I(x) \rangle - \langle |N(x)|^2 \rangle] e^{-i2\pi x \mu} dx. \quad (7)$$

Hence it is highly convenient to analyze closely the expression for $\langle H_Q(\mu) \rangle$. If we substitute Eq. (2) in Eq. (5) we obtain

$$\langle H_Q(\mu) \rangle = \int_{\frac{(2\Omega-\mu)}{2}}^{\frac{(2\Omega+\mu)}{2}} Q\left(\nu + \frac{\mu}{2}\right) Q\left(\nu - \frac{\mu}{2}\right) G\left(-\frac{2\mu\nu}{\Omega^2}\right) d\nu. \quad (8)$$

In Eq. (8) we use the Fourier transform of the acquisition function

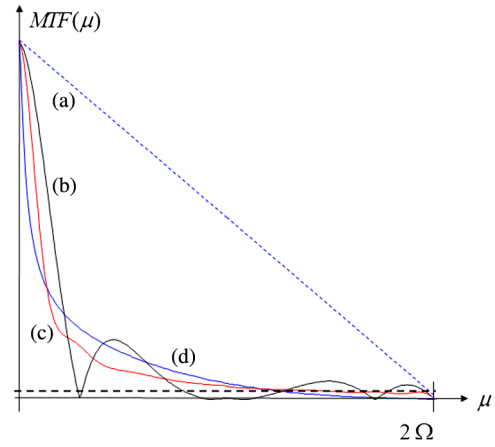


Fig. 2. (Color online) MTFs of (a) diffraction limited aperture, (b) focus error $W = 1$, (c) the average MTF, and (d) cubic phase mask and a Gaussian apodizer.

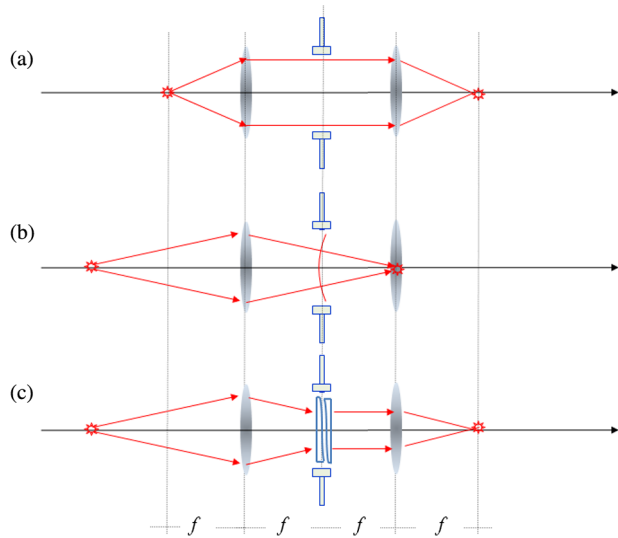
$$G\left(-\frac{2\mu\nu}{\Omega^2}\right) = \int_{-\infty}^{\infty} g(W) e^{-i2\pi\left(-\frac{2\mu\nu}{\Omega^2}\right)W} dW. \quad (9)$$

Consequently, $G(\cdot)$ plays the role of a characteristic function. From Eqs. (6)–(9), we recognize that by properly selecting the acquisition function, $g(W)$, one can achieve the two following goals. The function $g(W)$ shapes the additive noise average $\langle |N(x)|^2 \rangle$. And its Fourier transform $G(\cdot)$ engineers the average OTF. In this manner, one expects that our proposal will reduce the influence of additive noise and of focus errors.

In Fig. 2 we show the MTF of the following systems: (a) a diffraction limited aperture, (b) an optical system with focus error coefficient $W = 1$, (c) the average MTF associated with Eq. (6) for $Q(\mu) = 1$, and (d) an optical system with a cubic phase mask and a Gaussian apodizer [24]. It is apparent from Fig. 2 that for low frequencies, as well as for high frequencies, the average MTF has higher values than the MTF associated with a cubic phase mask working with a Gaussian apodizer. However, for the middle section of the spatial frequencies, the reverse is true. In the presence of white noise, it is convenient to consider minimum values of the MTF, as is depicted with a horizontal line in Fig. 2. In Section 4, we discuss the use of a threshold line in the MTF, for indicating that the values of the MTF should be above the influence of white noise. From Fig. 2, it is apparent that the methods labeled as (c) and (d) reach the threshold line at the same spatial frequency.

3. Tuning the Amount of Focus Error

As depicted in Fig. 3, we propose to use as spatial filter an Alvarez–Lohmann pair [29–32], which will transform a spherical wavefront into a plane wavefront, while preserving a fixed detection plane and a fixed magnification. In this manner, one can compensate the focus error associated with planes located outside the input plane. Or equivalently, one can select a given plane [out of a three-dimensional



F3:1 Fig. 3. (Color online) Varifocal lens for controlling the focus error
F3:2 coefficient.

180 (3-D) input], which will be imaged, at the fixed out-
181 put plane, with a focus error coefficient equal to zero.
182 In mathematical terms, for an Alvarez–Lohmann
183 pair, the complex amplitude transmittance is

$$T(\mu; \eta) = \exp \left\{ -i2\pi a \left[\left(\frac{\mu + \frac{\eta}{2}}{\Omega} \right)^3 - \left(\frac{\mu - \frac{\eta}{2}}{\Omega} \right)^3 \right] \right\} \text{rect} \left(\frac{\mu}{2\Omega} \right) \\ = \exp \left\{ -i \left(\frac{\pi}{2} \right) \left(\frac{\eta}{\Omega} \right)^3 \right\} \exp \left\{ -i2\pi \left(\frac{3a\eta}{\Omega} \right) \left(\frac{\mu}{\Omega} \right)^2 \right\} \\ \times \text{rect} \left(\frac{\mu}{2\Omega} \right). \quad (10)$$

184 In Eq. (10) we use a for denoting the optical path dif-
185 ference of the cubic phase elements forming the
186 Alvarez–Lohmann pair. We note that the complex
187 amplitude transmittance of one element is equal to
188 the complex conjugate of the other element [23].
189 The Greek letter η stands for a relative lateral dis-
190 placement (as a spatial frequency variable) between
191 the optical elements forming the pair. Hence, the
192 generalized pupil function of the optical processor is

$$P(\mu; \eta; W) = Q(\mu) T(\mu; \eta) e^{i2\pi W \left(\frac{\mu}{\Omega} \right)^2} \text{rect} \left(\frac{\mu}{2\Omega} \right). \quad (11)$$

193 Or equivalently,

$$P(\mu; \eta; W) = e^{i \left(\frac{\pi}{2} \right) \left(\frac{\eta}{\Omega} \right)^3} Q(\mu) e^{i2\pi \left[W - \frac{3a\eta}{\Omega} \right] \left(\frac{\mu}{\Omega} \right)^2} \text{rect} \left(\frac{\mu}{2\Omega} \right). \quad (12)$$

194 From Eq. (12), one can recognize that by changing
195 the relative lateral displacement η one can control
196 the focal length of the pair. And then, one can com-
197 pensate a specific amount of focus error by setting

$$\eta = \left(\frac{\Omega}{3a} \right) W. \quad (13)$$

198 Equivalently, one can select a certain plane, which is
199 associated with a specific value of W . This particular
200 plane is imaged (at the fixed detection plane) with
201 zero focus error. By using this technique, one can con-
202 trol the focus error coefficient without moving the op-
203 tical system. By using simple paraxial, ray tracing
204 formulas, one can show that the proposed device does
205 not change the lateral magnification of the optical
206 processor.

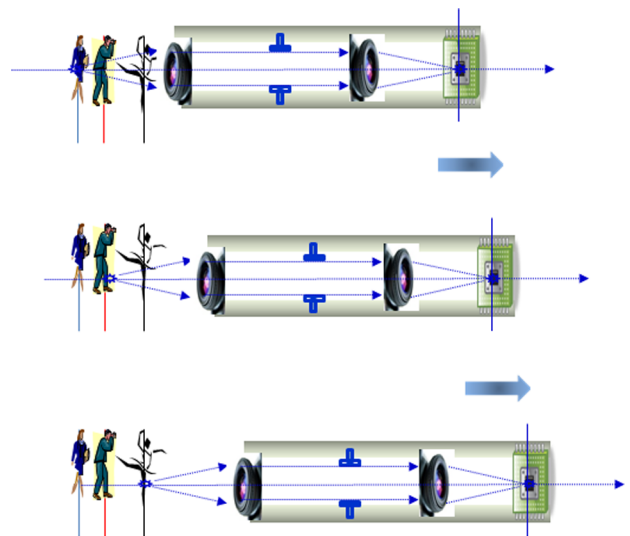
4. Useful Comparisons

207 Hauesler's pioneering proposal is illustrated in Fig. 4.
208 This proposal considers superimposing photographs
209 on the same film for an infinite range of focus error
210 coefficients. This ideal model is clearly limited by the
211 film dynamic range. However, one can argue that this
212 proposal generates a MTF that remains the same for
213 all out-of-focus image planes. This is indeed the main
214 characteristic of the preprocessing masks, which gen-
215 erate a MTF that does not vary for $0 \leq W \leq 3$.
216

217 Next, we use Fig. 5 for noting the following inter-
218 esting analogy between modulated exposure time
219 photography and our proposal. In Fig. 5 we show
220 that the snapshots are taken at equidistant values
221 in time. At a given time, say t_n , the focus error
222 coefficient is W_n , and the image irradiance distri-
223 bution is $I(x; W_n)$. Then, the exposure of the n -fold
224 snapshot is

$$E(x, t_n; W_n) = M(t_n) I(x, W_n). \quad (14)$$

225 In Eq. (14) we denote as $M(t_n)$ the relative factor de-
226 scribing the time that the pupil aperture remains
227 open recording the same frame $I(x; W_n)$. Next, we
228 consider that one selects the focus error coefficient,
229 as a function of time, with the following relationship:



F4:1 Fig. 4. (Color online) Hauesler proposal for extending the depth
F4:2 of field.

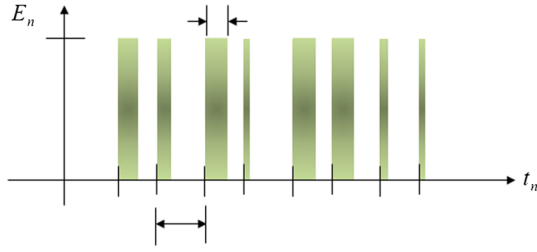


Fig. 5. (Color online) Weighting factors in modulated time photography.

$$W_n = f(t_n); \quad \text{or equivalently} \quad t_n = f^{-1}(W_n). \quad (15)$$

The last term in Eq. (15) indicates the inverse relationship that specifies the time as a function of the specific value of W_n . Next, we substitute the last term of Eq. (15) in Eq. (14) for obtaining

$$E(x, t_n; W_n) = M(f^{-1}(W_n))I(x, W_n) = g(W_n)I(x, W_n). \quad (16)$$

It is apparent from Eq. (16) that our proposed procedure can be linked to modulate exposure photography, if the acquisition function $g(W)$ is used for describing the time that the pupil aperture remains open when recording the frame $I(x; W_n)$.

Now, we consider some tolerance criteria. By closing down the pupil aperture, from a cutoff spatial frequency Ω to the cutoff spatial $\varepsilon\Omega$ (with $0 < \varepsilon \leq 1$) the Strehl ratio is

$$s(W) = \frac{I(x; W)}{I(0; 0)} = \text{sinc}^2(W\varepsilon^2). \quad (17)$$

Hence, one can use Eq. (17) for setting Rayleigh tolerance condition $s(W) \geq 0.8$, which leads to the values in Table 1. The equivalent ratio when using the MTF is

$$R(\mu; W) = \frac{|H_Q(\mu; W)|}{|H_Q(\mu; 0)|}. \quad (18)$$

The result in Eq. (18) was first proposed by Hopkins [26] for setting tolerances to wave aberrations in terms of the MTF. Here, we restrict our discussion to the influence of a focus error on a pupil aperture described by a rectangular function with cutoff spatial frequency $\varepsilon\Omega$. In this case Eq. (18) becomes

$$\begin{aligned} R(\mu; W) &= \frac{|H_Q(\mu; W)|}{|H_Q(\mu; 0)|} \\ &= \text{sinc}^2 \left[8(W\varepsilon^2) \left(\frac{\mu}{2\varepsilon\Omega} \right) \left(1 - \left| \frac{\mu}{2\varepsilon\Omega} \right| \right) \right]. \end{aligned} \quad (19)$$

Following Hopkins, the classical tolerance criteria should be expressed as $R(\mu; W) \geq 0.8$. However, for describing the methods that extend the depth of

field beyond the Rayleigh limit, we need a MTF that is different from zero inside its passband. For this case the requirement should be $R(\mu; W) > 0$. This is valid provided that one neglects the presence of noise.

However, in the presence of white noise, it is convenient to consider a detection threshold line, as is depicted in Fig. 2. When plotting the MTF, this threshold line indicates the values of the MTF that are above the noise level. And consequently, here we suggest to use Eq. (19) in the following form:

$$\text{sinc}^2 \left[8(W\varepsilon^2) \left(\frac{\mu}{2\varepsilon\Omega} \right) \left(1 - \left| \frac{\mu}{2\varepsilon\Omega} \right| \right) \right] \geq L. \quad (20)$$

The letter L denotes the values of the MTF that are above the threshold level, with the purpose of reducing the impact of white noise. For example, if one assumes the pupil aperture is reduced from Ω to $\varepsilon\Omega$, with $\varepsilon > 0.5$, and if one is interested at the middle of the passband, $\mu = \Omega$, then Eq. (21) becomes

$$\text{sinc}^2[W(2\varepsilon - 1)] \geq L. \quad (21)$$

By setting the white noise level below $L = 0.1$, the condition in Eq. (21) becomes

$$(2\varepsilon - 1)W = (2\varepsilon - 1) \frac{W_{2.0}}{\lambda} \leq 0.9, \quad \text{or} \quad W_{2.0} \leq \frac{9\lambda}{10(2\varepsilon - 1)}. \quad (22)$$

From Eq. (22) we recognize in an analytical fashion that the tolerance to focus error increases as one reduces the pupil aperture with a reduction ratio ε , such that $0.5 < \varepsilon \leq 1$. Of course, one should keep in mind that the light throughput decreases as ε^2 . We note that Eq. (20) can be applied for setting focus error tolerances for other spatial frequency values. Furthermore, Eq. (22) is useful for making comparisons (between proposals for extending the depth of field) for a given threshold value L .

5. Illustrative Examples

Now, for illustrating our previous formalism, next we discuss two simple applications, which are associated with the clear pupil aperture, $Q(\mu) = 1$. For the first case, we consider a set of consecutive snapshots, at random values of W , by using the following acquisition function:

$$g(W) = \left(\frac{1}{M} \right) \sum_{m=0}^{M-1} C_m \delta(W - W_m). \quad (23)$$

Trivially, the Fourier transform of Eq. (23) is

$$G\left(-\frac{2\mu\nu}{\Omega^2}\right) = \left(\frac{1}{M} \right) \sum_{m=0}^{M-1} C_m e^{i2\pi \left(\frac{2\mu\nu}{\Omega^2} \right) W_m}. \quad (24)$$



F6:1 Fig. 6. Averaging 10 snapshots having focus error coefficients
F6:2 with random values.

293 From Eqs. (8) and (24) it is straightforward to obtain
294 the average OTF

$$\langle H_Q(\mu) \rangle = \left(\frac{1}{M} \right) \sum_{m=0}^{M-1} C_m H_Q(\mu; W_m). \quad (25)$$

295 As expected, the average OTF results from superim-
296 posing M out-of-focus versions of the original OTF,
297 using as weighting factors the C_m coefficients. For
298 a few snapshots, the coefficients C_m have a strong im-
299 pact on the average. In Fig. 6, we illustrate the re-
300 sults of our proposal when taking 10 snapshots of
301 two sets of pictures as we change randomly the focus
302 error coefficient. For the first set we use as input a

303 Siemens star. For the second set we employ a picture
304 of Lena. From left to right, along the two lines of
305 Fig. 6, the focus error coefficient changes as follows:
306 $W = 0.3569, 0.4878, 0.6714, 0.8280, 1.0212, 1.4951,$
307 $1.7578, 1.9653, 2.0391,$ and 2.8992 . The average im-
308 age appears at the bottom of Fig. 6: We note that the
309 final average image exhibits a “soft focus” effect,
310 which was not part of our searching the goals. The
311 soft focus effect can be reduced if one uses digital
312 algorithms for enhancing the picture.

313 Now, related to the experimental results in
314 Ref. [27], next we consider a continuous variation
315 on the values of W . We show that the proposed ana-
316 lytical approach gives some insights on the selection
317 of the acquisition function. Let us consider that

$$g(W) = \left(\frac{1}{W_{\max}} \right) \text{rect} \left(\frac{W}{W_{\max}} \right). \quad (26)$$

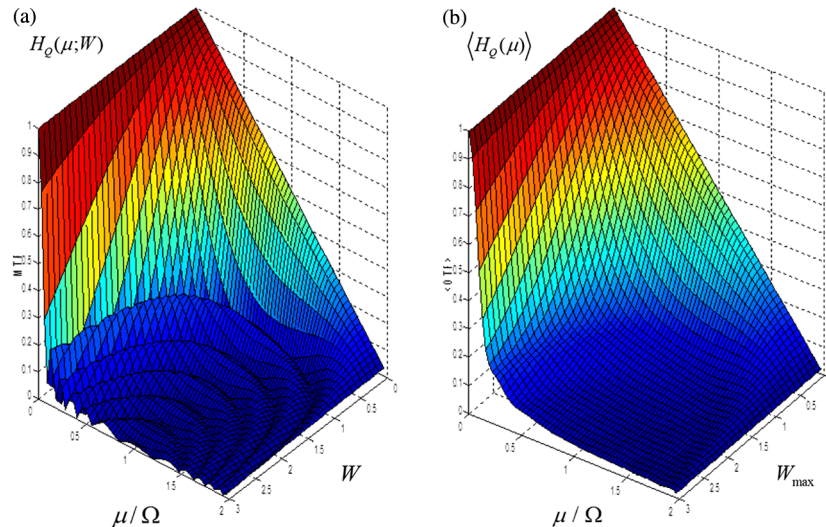
The Fourier transform of the above acquisition func-
318 tion is
319

$$G \left(-\frac{2\mu\nu}{\Omega^2} \right) = \text{sinc} \left(\frac{2\mu\nu W_{\max}}{\Omega^2} \right). \quad (27)$$

Hence, for a clear pupil aperture $Q(\mu) = 1$, we have
320 that
321

$$\langle H_Q(\mu) \rangle = \frac{1}{8\pi \left(\frac{\mu}{2\Omega} \right) W_{\max}} \text{Si} \left(8\pi \left(\frac{\mu}{2\Omega} \right) \left(1 - \left| \frac{\mu}{2\Omega} \right| \right) W_{\max} \right). \quad (28)$$

322 In Eq. (28) we use the common notation $\text{Si}(\cdot)$ for the
323 sine integral (SI) function as in Ref. [27]. From
324 Eq. (28) one can recognize that the average OTF
325 is a nonmonotonic function. In Fig. 7(a) we show a
326 3-D display of the MTF for the clear pupil. The
327 3-D graph in Fig. 7(b) displays the variations of
328 $\langle H_Q(\mu) \rangle$ as we change the maximum value of the



F7:1 Fig. 7. (Color online) MTF versus focus error and average MTF versus maximum integration value.

focus error coefficient, which varies from 0.01 to 3.0. It is apparent from Fig. 7 that the average OTF does reduce the impact of focus errors. Next, from Eq. (28) we note that, furthermore, for a continuous variation on the values of W , and if one selects a specific spatial frequency value, say $\mu = \sigma > 0$, the SI function reaches its maximum value at

$$W_{\max} = \frac{1}{8\left(\frac{\sigma}{2\Omega}\right)\left(1 - \frac{\sigma}{2\Omega}\right)}. \quad (29)$$

For example, if we select the spatial frequency at the middle of the passband, $\sigma = \Omega$, then according to Eq. (29) $W_{\max} = 0.5$, which corresponds to $W_{2,0} = \lambda/2$, which is a feasible task. Hence, from Eq. (28) we claim that when superimposing snapshots from $W = 0$ to $W = 0.25$, at $\mu = \Omega$, the MTF reaches the value $\langle H_Q(\mu) \rangle = 0.25$.

6. Final Remarks

We have proposed a simple optical technique for extending the depth of the field at full pupil aperture by superimposing several out-of-focus snapshots. Since at every snapshot one changes the axial separation between the input plane and the output plane, it was relevant to discuss an optical method for changing the focus error coefficient. We presented the use of an Alvarez–Lohmann pair in an optical processor for controlling the focus error coefficient without modifying either the lateral magnification or the light throughput.

We have indicated that if in the Fourier domain the noise is a wide-sense stationary process, then when superimposing snapshots the additive noise averages to a constant value. If, however, in the Fourier domain the noise is white, then we have suggested using Hopkins tolerance formalism for setting threshold values in the MTF.

We have reported simple numerical simulations that validate our proposal. Our discussions do not include state-of-the-art techniques for digital recording and processing.

Appendix A

According to Eq. (5) in the main text, at the recording stage, the additive noise is $|N(x; W)|^2$. Its ensemble average is defined as

$$\langle |N(x)|^2 \rangle = \int_{-\infty}^{\infty} g(W) |N(x; W)|^2 dW. \quad (A1)$$

Now, the Fourier spectrum of Eq. (A1) is

$$\begin{aligned} P(\mu) &= \int_{-\infty}^{\infty} \langle |N(x)|^2 \rangle e^{-i2\pi\mu x} dx \\ &= \int_{-\infty}^{\infty} g(W) \int_{-\infty}^{\infty} N(x; W) N^*(x; W) e^{-i2\pi\mu x} dx dW. \end{aligned} \quad (A2)$$

By employing the autocorrelation theorem of the Fourier transform, one can rewrite Eq. (A2) as

$$\begin{aligned} P(\mu) &= \int_{-\infty}^{\infty} g(W) \int_{-\infty}^{\infty} \tilde{N}\left(\nu + \frac{\mu}{2}; W\right) \tilde{N}^* \left(\nu - \frac{\mu}{2}; W\right) d\nu dW \\ &= \int_{-\infty}^{\infty} \left\langle \tilde{N}\left(\nu + \frac{\mu}{2}\right) \tilde{N}^*\left(\nu - \frac{\mu}{2}\right) \right\rangle d\nu. \end{aligned} \quad (A3)$$

We recognize next that the last term in Eq. (A3) is the autocorrelation of a stochastic process. As is discussed in Ref. [33], for a wide-sense stationary process, the autocorrelation of a stochastic process is proportional to a Dirac's delta. That is, $P(\mu) = N_0 \delta(\mu)$, where N_0 is a constant. The inverse Fourier transform of $P(\mu)$ is $\langle |N(x)|^2 \rangle$, which is equal to the constant N_0 .

We are indebted to CoNaCyT for the research Grant No. 157673 and to PROMEP for Grant Nos. 12345 and PTC-197 D. We extend our gratitude to the reviewers for useful suggestions.

References

1. M. Mino and Y. Okano, "Improvement in the OTF of a defocused optical system through the use of shaded apertures," *Appl. Opt.* **10**, 2219–2225 (1971).
2. J. Ojeda-Castañeda, L. R. Berriel-Valdos, and E. L. Montes, "Line-spread function relatively insensitive to defocus," *Opt. Lett.* **8**, 458–460 (1983).
3. J. Ojeda-Castañeda, L. R. Berriel-Valdos, and E. Montes, "Spatial filter for increasing the depth of focus," *Opt. Lett.* **10**, 520–522 (1985).
4. J. Ojeda-Castañeda, P. Andrés, and A. Díaz, "Annular apodizers for low sensitivity to defocus and to spherical aberration," *Opt. Lett.* **11**, 487–489 (1986).
5. J. Ojeda-Castañeda and L. R. Berriel-Valdos, "Arbitrarily high focal depth with finite apertures," *Opt. Lett.* **13**, 183–185 (1988).
6. J. Ojeda-Castañeda, L. R. Berriel-Valdos, and E. Montes, "Ambiguity function as a design tool for high focal depth," *Appl. Opt.* **27**, 790–795 (1988).
7. J. Ojeda-Castañeda and A. Noyola-Isgleas, "High focal depth by apodization and digital restoration," *Appl. Opt.* **27**, 2583–2586 (1988).
8. J. Ojeda-Castañeda and A. Díaz, "High focal depth by quasi-bifocus," *Appl. Opt.* **27**, 4163–4165 (1988).
9. E. R. Dowski and T. W. Cathey, "Extended depth of field through wave-front coding," *Appl. Opt.* **34**, 1859–1865 (1995).
10. H. Wang and F. Gan, "High focal depth with a pure-phase apodizer," *Appl. Opt.* **40**, 5658–5662 (2001).
11. S. Sanyal and A. Ghosh, "High tolerance to spherical aberrations and defects of focus with a birefringent lens," *Appl. Opt.* **41**, 4611–4615 (2002).
12. N. George and W. Chi, "Extended depth of field using a logarithmic asphere," *J. Opt. A* **5**, s157–s163 (2003).
13. A. Saucedo and J. Ojeda-Castañeda, "High focal depth with fractional-power wave fronts," *Opt. Lett.* **29**, 560–562 (2004).
14. A. Castro and J. Ojeda-Castañeda, "Asymmetric phase masks for extended depth of field," *Appl. Opt.* **43**, 3474–3479 (2004).
15. S. S. Sherif, W. T. Cathey, and E. R. Dowski, "Phase plate to extend depth of field of incoherent hybrid imaging system," *Appl. Opt.* **43**, 2709–2721 (2004).
16. J. Ojeda-Castañeda, J. E. A. Landgrave, and H. M. Escamilla, "Annular phase-only mask for high focal depth," *Opt. Lett.* **30**, 1647–1649 (2005).

17. A. Castro, J. Ojeda-Castaneda, and A. W. Lohmann, "Bow-tie effect: differential operator," *Appl. Opt.* **45**, 7878–7884 (2006).
18. S. Mezouari, G. Muyo, and A. R. Harvey, "Circularly symmetric phase filters for control of primary third-order aberrations: coma and astigmatism," *J. Opt. Soc. Am. A* **23**, 1058–1062 (2006).
19. G. Mikula, Z. Jaroszewicz, A. Kolodziejczyk, K. Petelczyc, and M. Sypek, "Imaging with extended focal depth by means of lenses with radial and angular modulation," *Opt. Express* **15**, 9184–9193 (2007).
20. M. Somayaji and M. P. Christensen, "Frequency analysis of the wavefront-coding odd-symmetric quadratic phase mask," *Appl. Opt.* **46**, 216–226 (2007).
21. Y. Takahashi and S. Komatsu, "Optimized free-form phase mask for extension of depth of field in wavefront-coding imaging," *Opt. Lett.* **33**, 1515 (2008).
22. N. Caron and Y. Sheng, "Polynomial phase masks for extending the depth of field of a microscope," *Appl. Opt.* **47**, E39–E43 (2008).
23. J. Ojeda-Castañeda, J. E. A. Landgrave, and C. M. Gómez-Sarabia, "The use of conjugate phase plates in the analysis of the frequency response of optical systems designed for an extended depth of field," *Appl. Opt.* **47**, E99–E105 (2008).
24. J. Ojeda-Castañeda and C. M. Gómez-Sarabia, "Optical processor arrays for controlling focal length or for tuning the depth of field," *Photonics Lett. Pol.* **3**, 44–46 (2011).
25. J. Ojeda-Castañeda, E. Yépez-Vidal, and E. García-Almanza, "Complex Amplitude Filters for Extended Depth of Field," *Photon. Lett. Pol.* **2**, 162–164 (2010).
26. H. H. Hopkins, "The aberration permissible in optical systems," *Proc. Phys. Soc. B* **70**, 449–470 (1957).
27. G. Haeusler, "A method to increase the depth of focus by two step image processing," *Opt. Commun.* **6**, 38–42 (1972).
28. R. Raskar, A. Agrawal, and J. Tumblin, "Coded exposure photography: motion deblurring via fluttered shutter," *SIGGRAPH* (2006).
29. L. W. Alvarez, "Two-element variable-power spherical lens," U. S. Patent 3,305,294 (3 December 1964).
30. A. W. Lohmann, "Lente focale variabile," Italian Patent 727, 848 (19 June 1964).
31. A. W. Lohmann, "Improvements relating to lenses and to variable optical lens systems formed by such lenses," Patent Specification 998,191, The Patent Office, London (1965).
32. A. W. Lohmann, "A new class of varifocal lenses," *Appl. Opt.* **9**, 1669–1671 (1970).
33. B. R. Frieden, *Probability, Statistical Optics and Data Testing* (Springer-Verlag, 1991), pp. 182–183.

Queries

1. AU: The OCIS code has been changed from “110.688” to “110.6880”. Please check and confirm
2. AU: Since Tables 1 and 2 are really images, it may be better to label them as figures. Please reorder figures so all are cited in text in numerical order.
3. AU: Please define PSF.
4. AU: Please provide complete publication information for Ref. [28].
5. AU: Please provide day and month for Ref. 31